Fluorescence Characteristics of Blue Amber from the Dominican Republic, Mexico, and Myanmar

Zhiqing Zhang, Xinran Jiang, Yamei Wang, Fanli Kong, and Andy H. Shen

Amber shows various luminescence phenomena under UV illumination. Amber with very strong blue fluorescence under sunlight or D65 illumination can appear blue to the unaided eye when placed on a black background. Amber showing this effect is highly sought after in the Chinese gem market and referred to as "blue amber." Almost all commercial blue amber is mined from the Dominican Republic, Mexico, and Myanmar. In this study, we collected and characterized the appearance, gemological properties, UV-visible light absorption spectra, and 3D fluorescence spectra of blue amber from these three producing areas. The results show that blue amber from the Dominican Republic generally emits much stronger fluorescence than the other two origins, with narrow triple-peak emissions near 450, 474, and 508 nm. Mexican and Burmese excitation-emission maps present several distinct emission and excitation wavelengths. Additionally, distinctive UV/visible/near-infrared absorptions at 412 and 441 nm appeared only in blue amber from the Dominican Republic. The combination of appearance, UV-Vis-NIR spectroscopy, and excitation-emission mapping may assist in the separation of blue amber from these three localities.

Amber is widely distributed around the world. It is of interest not merely as an important natural fossil resin witnessing the history of the earth and providing direct evidence for paleobiologists, but also as a widely loved organic gemstone. Transparent yellow amber from the Dominican Republic, Mexico, and Myanmar displaying a blue or greenish blue glow when viewed on a black background in normal sunlight is called "blue amber" in the Chinese gem trade. This paper focuses on amber displaying this characteristic and will refer to this material as blue amber. In the Guangzhou and Shenzhen amber trading centers, Dominican blue amber can be sold for up to thousands of Chinese RMB (around several hundred U.S. dollars) per gram, while Mexican material fetches only several hundred RMB (around several tens of U.S. dollars) per gram—even though they have a similar appearance.

Bellani et al. (2005) first described blue amber and studied the fluorescence emission, excitation, and optical absorption spectra of Dominican blue and non-blue (including yellow and red varieties) amber. They found that multiple emission fluorescence peaks at 449 nm, 476 nm, and 505 nm occurred in this blue amber, while only a broad fluorescence band was observed in non-blue amber. They further proposed that perylene (a polycyclic aromatic hydrocarbon, $C_{20}H_{12}$) was the fluorophore for Dominican blue amber by comparing the emission spectra and

In Brief

- Amber that shows strong blue fluorescence under daylight is called "blue amber" in the Chinese gem market. These can be classified into blue and blue-green groups.
- The main production areas are the Dominican Republic, Myanmar, and Mexico.
- 3D fluorescence spectroscopy showed distinct features among these groups and localities.
- The combination of appearance, UV-Vis-NIR spectroscopy, and excitation-emission mapping may assist in the separation of blue amber from these three localities.

See end of article for About the Authors and Acknowledgments.
Gems & Gemology, Vol. 56, No. 4, pp. 484–496,
http://dx.doi.org/10.5741/GEMS.56.4.484

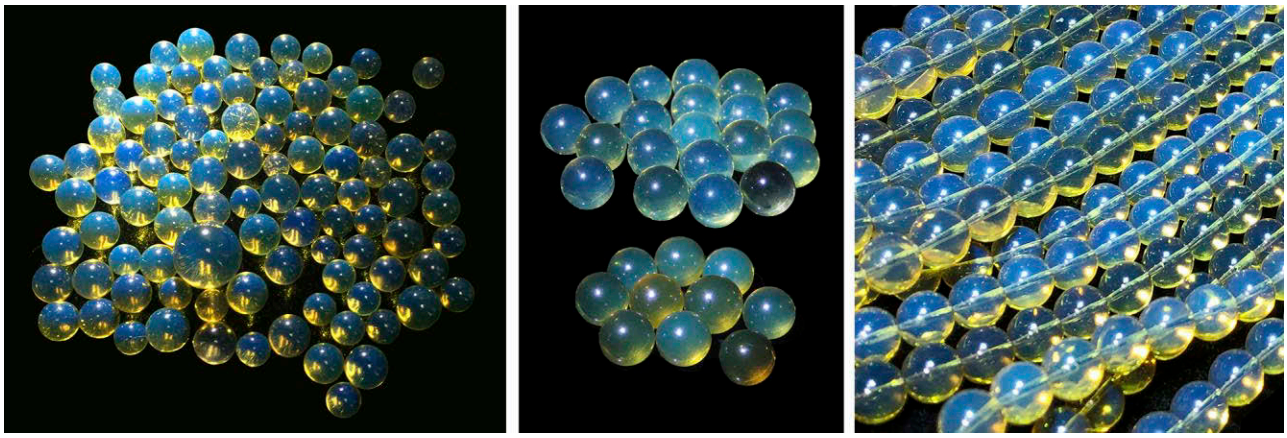

Figure 1. Commercial blue amber beads from the Dominican Republic (left, about 6–15 mm in diameter), Mexico (center, approximately 10 mm), and Myanmar (right, approximately 5 mm) have very similar appearances. The illumination source is a handheld D65 light. Photos by Y. Wang.

fluorescence lifetime with the fluorescence spectra documented in the handbook by Berlman (1971). Liu et al. (2014) found blue amber's fluorescence to be confined to the surface, and further illustrated that a black background could enhance the visibility of the fluorescence by reducing the amount of scattered light that reaches the eye. Chekryzhov et al. (2014) and Bechtel et al. (2016) discussed the luminescence properties and the hydrocarbon composition of blue amber from the Russian Far East, but they did not give a possible cause of the blue fluorescence. Recently, Jiang et al. (2017) analyzed the fluorescence emission wavelengths and optimal excitation wavelengths, aiming to distinguish Dominican from Mexican and Burmese blue amber. Additionally, the fluorescence properties of Baltic Sea and Ukrainian amber have been described using conventional and synchronous fluorescence spectrometers (Matuszewska and Czaja, 2002; Mysiura et al., 2017).

The main purpose of this work is to fully characterize blue amber from the Dominican Republic, Mexico, and Myanmar, as well as to compare their gemological properties, UV-Vis-NIR spectra, and 3D fluorescence spectra. To make the following discussion more applicable to practical identification workflow, we classify these amber samples according to their apparent fluorescence colors (blue, greenish blue, and non-blue) and then discuss the difference in EEM (also known as 3D fluorescence spectra, excitation-emission matrix, or excitation-emission mapping) from different origins in each category.

SAMPLES AND METHODS

Samples. For this study, we contacted merchants in the Chinese gem trade who dealt mainly with specific amber species and could provide samples with reliable origins as well as current market information. Figure 1 shows commercial blue amber beads from three sources. We tested a total of 247 amber specimens (including beads, fragments, and jewelry pieces) reportedly from the Dominican Republic (109), Mexico (47), and Myanmar (91).

Gemological Testing. Standard gemological and spectroscopic testing were all performed at the Gemmological Institute of China University of Geosciences (Wuhan). Specific gravity (SG) values were determined hydrostatically using a Sartorius BT 224 S balance. Refractive indices (RI) were measured with a GR-6 refractometer produced by Wuhan Xueyuan Jewelry Technology Co. Ltd. Reaction to long-wave ultraviolet light (LWUV: 365 nm) and short-wave ultraviolet light (SWUV: 254 nm) was observed using a standard handheld gemological 4W UV light source (mercury bulb), also made by Wuhan Xueyuan Jewelry Technology Co. Ltd. Samples and inclusions were observed and photographed using a Leica M205 A microscope and a Nikon D810 camera. For each bead, two sets of images were captured—one on a white background and the other on a black background, to show the difference in appearance.

UV-Vis-NIR Spectroscopy. UV/visible/near-infrared absorption spectra were measured in transmission mode with a PerkinElmer Lambda 650 S spectrophotometer. Spectral scans were collected from 250 to 800 nm with a speed of 266.75 nm/min and a data interval of 1.00 nm. The detector response was set at 0.2 s. To successfully perform transmission spectroscopy, the samples needed to be prepared as slices;

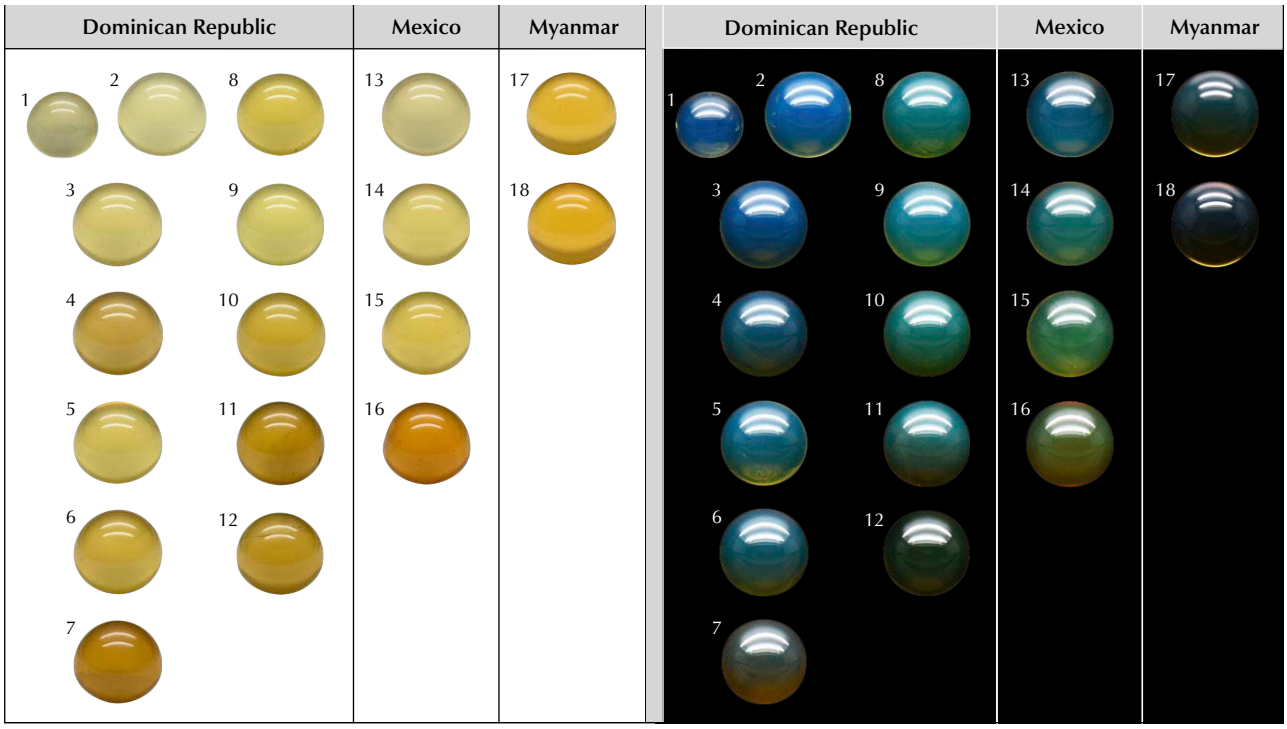

Figure 2. Assembled photos of selected samples representing various types of amber discussed in the text. The photos on the left were taken in a light box under D65 illumination with the samples placed on a standard white background, and those on the right were taken in a light box under D65 illumination with the samples placed on a black velvet background. All photos have variable magnification for optimal display. Samples 1–12 are from the Dominican Republic (B-type: 1–7, GB-type: 8–11, NB-type: 12); samples 13–16 are from Mexico (B-type: 13–14, GB-type: 15–16); and samples 17 and 18 are from Myanmar (B-type). Photos by Z. Zhang.

all slices were less than 0.5 mm in thickness. It is not possible to perform this type of destructive testing on samples intended for jewelry.

Fluorescence Spectroscopy. All fluorescence spectra were recorded at room temperature using a Jasco FP-8500 fluorescence spectrometer (see box A). 3D fluorescence spectral data (i.e., EEM) was collected with a 2000 nm/min scan speed. The excitation wavelengths varied from 220 to 500 nm, with a step size of 5 nm and an excitation bandwidth of 5 nm. The emission spectra were collected with a starting wavelength 10 nm longer than the excitation wavelength and up to 750 nm, with the bandwidth set to 5 nm and a data interval of 1 nm. The beam size was fixed with a 3 mm diameter aperture. In order to keep the illuminated area constant, the sample was placed in a fixed position in a sample holder with a 2 mm diameter opening (see figure A-2). Each EEM, made up of 57 individual emission scans, usually took about 20 minutes to collect. The final EEM spectra appeared similar to a contour map with color coding to indicate the strength of the fluorescence emission peaks or bands under various excitation wavelengths (see box B).

After identifying the main emission peaks, specific excitation wavelengths were chosen and finer-resolution emission scans were performed to obtain more detailed spectra for these specific excitation wavelengths. These scans were conducted with the excitation bandwidth set to 2.5 nm, emission bandwidth 1 nm, and the data interval 1 nm.

Data Collection. All data were recorded using Spectra Manager II software from Jasco. The same software package was used to construct the EEMs from 57 rows and 511 columns of data; higher-resolution emission spectra were drawn as typical two-dimensional plots using plotting software.

RESULTS

Standard Gemological Properties. All samples were colorless to yellow to orange under a standard D65 light when placed on a white background, but the Burmese samples tended to have a richer yellow color. However, when viewed on a black background

BOX A: FLUORESCENCE SPECTROMETER AND EXPERIMENTAL GEOMETRY

Fluorescence spectroscopy has been applied to study the fluorescence of liquids and solid-state luminescent materials. The instrument is called a spectrofluorometer, and it records detailed information about the fluorescence emission spectrum under different excitation wavelengths as well as the excitation efficiency of a particular emission wavelength. This is done by fixing the emission wavelength and scanning through different excitation wavelengths (thus producing what is known as an excitation spectrum).

In a typical spectrofluorometer instrument for analyzing fluorescing liquids, the measurement geometry for the excitation beam, the sample, and the emission beam is set at 90° (Lakowicz, 2006; figure A-1). In this mode, the excitation light travels through the sample and the collected emission light travels through the same distance in the sample. The emission measured is the accumulation of the luminescence along the whole optical path, which is greatly affected by self-absorption and secondary fluorescence. Liu et al. (2014) pointed out that amber's fluorescence occurs mainly on the surface; therefore, a front-surface geometry determination can substantially remove the self-absorption and secondary fluorescence effect (Parker, 1968; Birks, 1974; Airado-Rodriguez et al., 2011).

We performed our experiment using a Jasco FP-8500 spectrofluorometer equipped with a 150 W xenon lamp and a special accessory (EFA-833). This accessory provides a preferred geometry for this study: front-surface mode with an incident angle (between the incident excitation beam and the normal of the sample surface) of approximately 45° (schematic shown in figure A-2). At the same time, no sample pre-treatment is required, which makes this a truly nondestructive test.

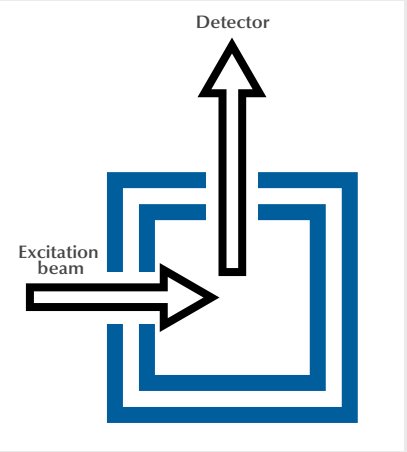

Figure A-1. Schematic of the geometric arrangement for observation of fluorescence in a classic spectrofluorometer (Lakowicz, 2006).

In the FP-8500 fluorescence spectrometer, the maximum emission intensity (I) is limited to 10000 arbitrary units (a.u.), and the actual measurement requires adjusting several measurement parameters such as the size of the slit on the accessory controlling the incident beam, the voltage on the photomultiplier (PMT), and other parameters. In our EEM measurements, all parameters were fixed manually so that the relative intensities of the fluorescence given out by each amber sample from the obtained spectra could be directly compared.

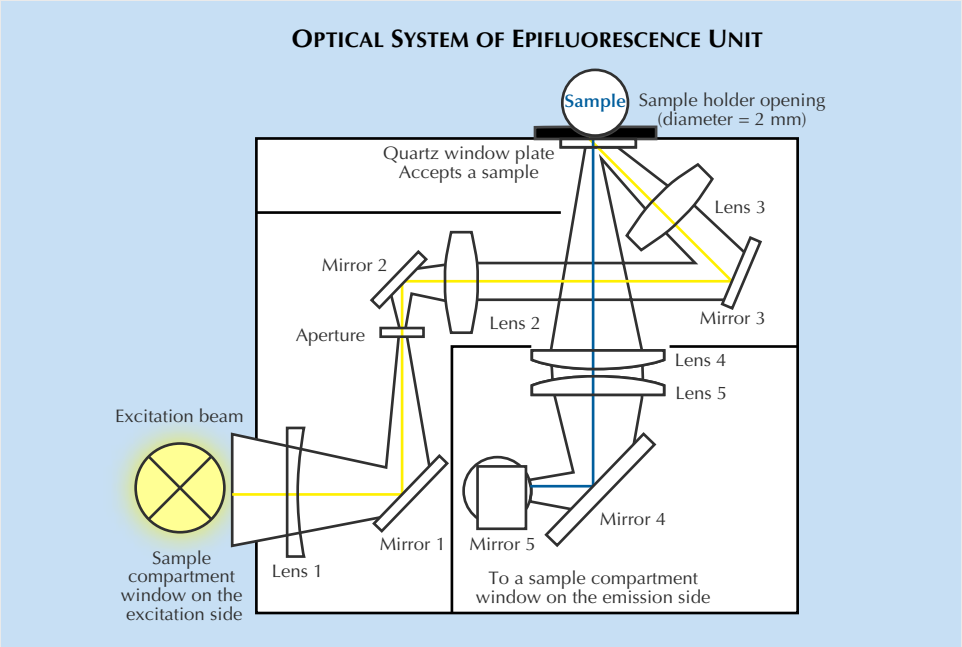

Figure A-2. Schematic of the EFA-833 optical accessory attached to the Jasco FP-8500 instrument used in this study (redrawn by Z. Zhang, from the Jasco FP-8500 handbook). We used a front-surface geometry to minimize the influence of self-absorption and secondary emission effects on measurements of solid samples. This geometry also accommodates gemstones.

Box B: 3D Fluorescence Spectra

3D fluorescence spectra are also known as excitation-emission matrices or excitation-emission maps (EEM). The data collection is conducted by starting with the shortest excitation wavelength and an emission scan from a wavelength 10 nm longer than the excitation wavelength to a set ending point. The excitation wavelength is increased by a set step size, and the emission scan is started again from a wavelength 10 nm longer than the new excitation wavelength to the ending wavelength. This is repeated until the set excitation wavelength range is complete. As shown in figure B-1, these data are commonly plotted in emission wavelength (nm) versus excitation wavelength (nm), with intensity (a.u.) as the third dimension, either plotted directly or referencing a color-coded contour map. In these maps, each horizontal cross section is an emission spectrum, which indicates the intensity distribution of emission wavelengths, measured at a single excitation wavelength. Each vertical cross section is an excitation spectrum, which shows the efficiency of emission by scanning through various excitation wavelengths, while holding constant at a single emission wavelength.

Some commonly encountered terms and their symbols for expressing characteristics of 3D fluorescence spectra used in the main text are presented in table B-1.

TABLE B-1. Summary of relevant terms and symbols.

Symbol	Meaning
λ_{em}	Emission wavelength
λ_{ex}	Excitation wavelength
$I_{\lambda em=450\ nm}$	Intensity of fluorescence at emission wavelength of 450 nm
$I_{\lambda em}$	Intensity of fluorescence at all emission wavelengths

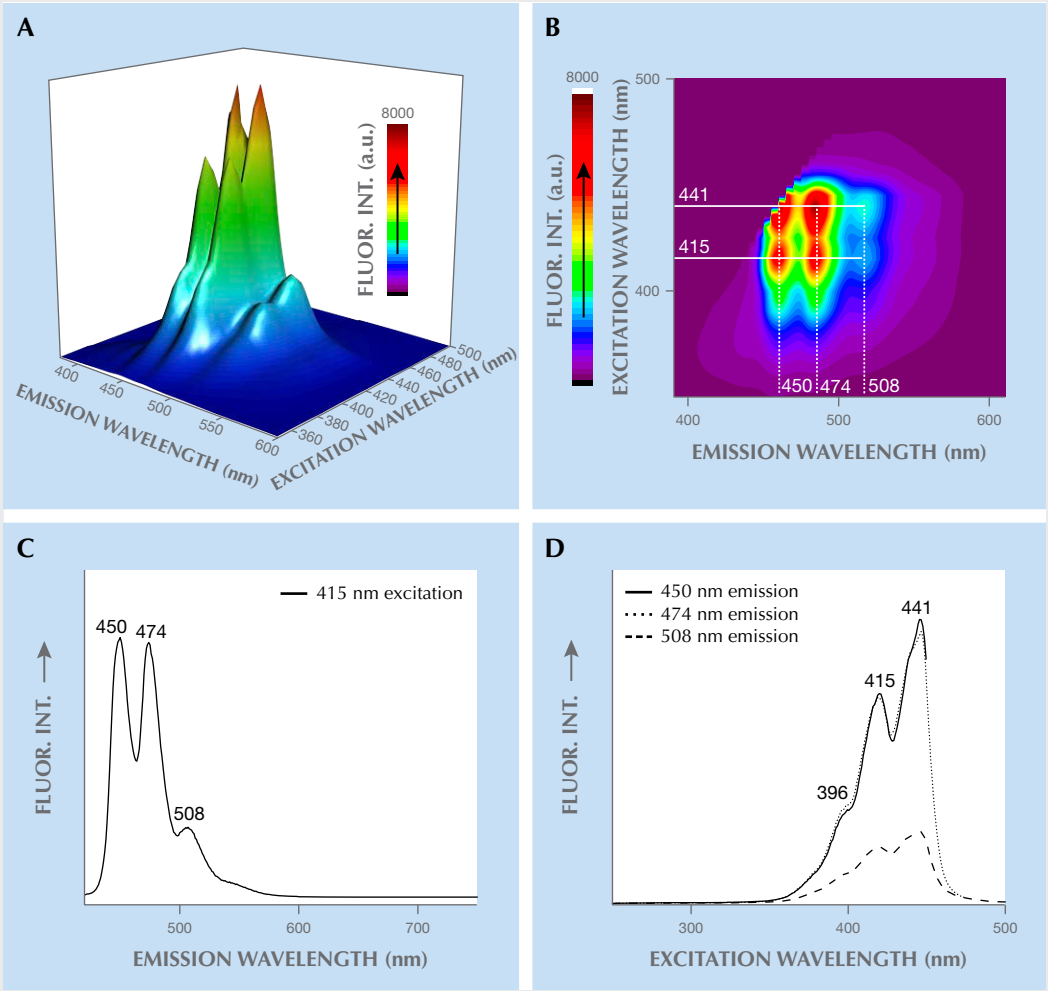

Figure B-1. The three-dimensional plot and contour map (A and B) from a Dominican blue amber fluorescence spectrum shows three extremal emission wavelengths at 450, 474, and 508 nm, and their corresponding optimal excitation wavelengths at 415 and 441 nm. Plots C and D present the emission curve and the excitation curves, respectively.

TABLE 1. Summary of gemological properties of all samples.

Locality	Dominican Republic	Mexico	Myanmar
Total no. of samples	109	47	91
No. of B-type	74	22	5
No. of GB-type	29	22	
No. of NB-type	6	3	86
Color observed on a white background	Colorless to yellow to orange	Colorless to yellow to orange	Yellow
Transparency	Transparent	Transparent	Transparent
SG	1.032–1.051	1.030–1.048	1.024–1.042
RI	1.54	1.54	1.54
Internal features	Usually clean. For all three sources, sporadic tiny red solid inclusions were observed. Some tiny bubbles were observed in Burmese samples.		
Fluorescence reaction	LWUV: Very strong to weak blue fluorescence	LWUV: Strong to weak blue fluorescence	LWUV: Medium violetish blue fluorescence
	SWUV: Weak blue fluorescence to inert	SWUV: Weak blue fluorescence to inert	SWUV: Weak violetish blue fluorescence to inert
Phosphorescence	Faint greenish yellow	Faint greenish yellow	Evident yellow

under a standard D65 light source, three types of color appearance were easily identified—blue fluorescence (B-type), greenish blue fluorescence (GB-type), and fluorescence that was too weak to see and thus labeled as non-blue amber (NB-type) (such as the examples seen in figure 2). Liu et al. (2014) attributed the color appearance change from yellow to blue to the superposition of the reflected light with its fluorescence. Most blue amber in the market has an evenly distributed blue or greenish blue color across the entire surface. Among all 247 samples we studied, we found that those from the Dominican Republic and Mexico included both B- and GB-types, while Myanmar had only B-type. NB-type amber occurred in all three sources.

Table 1 summarizes the samples by color appearance and the results of standard gemological testing. The RI values by spot measurement were all 1.54, while the SG values ranged from 1.032 to 1.051 for material from the Dominican Republic, 1.030 to 1.048 for material from Mexico, and 1.024 to 1.042 for material from Myanmar. When observed under the microscope, the samples were quite transparent, with a few tiny internal features. The fluorescence response was typically LWUV > SWUV, with or without the phosphorescence. Under LWUV illumination, Dominican and Mexican blue amber showed blue fluorescence, while the Burmese samples sometimes displayed a violetish blue fluorescence.

UV-Vis-NIR Spectroscopy. We collected in total 178 spectra from 81 Dominican amber samples (including 76 B- and GB-type, and 5 NB-type), 44 Mexican amber samples, and 53 Burmese amber samples. Typical UV-Vis-NIR absorption curves for blue amber are shown in figure 3. We noticed that the absorption edges of samples from all three origins were similarly located at about 400 nm. A tailing absorption from 400 to 500 nm indicates that when mixed-wavelength sunlight strikes blue amber, wavelengths shorter than 400 nm cannot penetrate deeply, while light between 400 and 500 nm may be able to penetrate a little deeper, resulting in a yellowish bodycolor. In Dominican blue amber samples, two distinctive absorption peaks occurred at 412 and 441 nm as well, thus further limiting the 400–450 nm light penetration for Dominican samples. These two peaks are distinctive features for blue amber from the Dominican Republic and were not detected in material from Mexico or Myanmar. However, both the size (or thickness) and the color of samples impact the detection results, so this test has its limitations in real-world gem testing.

Fluorescence Spectroscopy. A brief introduction to 3D fluorescence spectra (EEMs) and relevant terms and symbols are provided in box B.

After collecting 3D fluorescence spectra of all samples, totaling 247 EEM spectra, we found that the fluorescence intensity varied in different samples, while the excitation-emission maps had similar features for samples of the same type from the same origin. To describe blue amber fluorescence features in detail, we selected 18 samples (numbered and shown in figure

2), which had typical EEMs representing the various groups of all blue amber in this study. They included 11 pieces of B-type with different fluorescence intensity (samples 1–7 from the Dominican Republic, 13–14 from Mexico, and 17–18 from Myanmar); six beads of GB-type with different fluorescence intensity (samples 8–11 from the Dominican Republic and 15–16 from Mexico); and one non-blue amber (sample 12) from the Dominican Republic.

Fluorescence of B-Type Amber. Figure 4 compares the 3D fluorescence spectra and significant emission and excitation curves of B-type amber from the Dominican Republic, Mexico, and Myanmar.

From the EEMs of all Dominican B-type samples (74 specimens, figure 4A), we found that the fluorescence emission consisted of three peaks that were rather stable when excited by different excitation wavelengths. Figure 4B shows a typical emission spectrum using λ_{ex} = 415 nm; three main peaks at wavelengths of λ_{em} = 450, 474, and 508 nm are clearly visible. These three fluorescence peaks are in good agreement with those reported by Bellani et al. (2005), Chekryzhov et al. (2014), Liu et al. (2014), and Jiang et al. (2017). The observed fluorescence intensity $I_{\lambda em=450\ nm}$ is generally about the same as $I_{\lambda em=474\ nm}$, though it is sometimes a bit stronger. The strongest fluorescence emission can be excited by λ_{ex} = 415 and 441 nm, but the strongest λ_{em} is observed using 441 nm excitation (figure 4C). Additionally, λ_{em} can only be excited using λ_{ex} between 350 and 460 nm, thus explaining the somewhat inert reaction to SWUV.

Compared with their Dominican counterparts, all Mexican and Burmese B-type samples tended to have weaker $I_{\lambda em}$, as indicated by the lower maximum values for fluorescence intensity in their EEM spectra, as in figures 4A, 4D, and 4G. Their emission patterns were also rather different.

In Mexican B-type samples, shown in figure 4, D–F, when excited using λ_{ex} = 441 and 415 nm, one can see similar triple-peak patterns made up of 451, 476, and 514 nm emissions. Upon switching to a shorter excitation wavelength of λ_{ex} = 400 nm, two different emission bands appeared near 438 and 456 nm (figure 4E). Additionally, the most efficient excitation region in these samples was from 320 to 475 nm, which is rather far from the typical SWUV (254 nm radiation found in a handheld UV light source), thus resulting

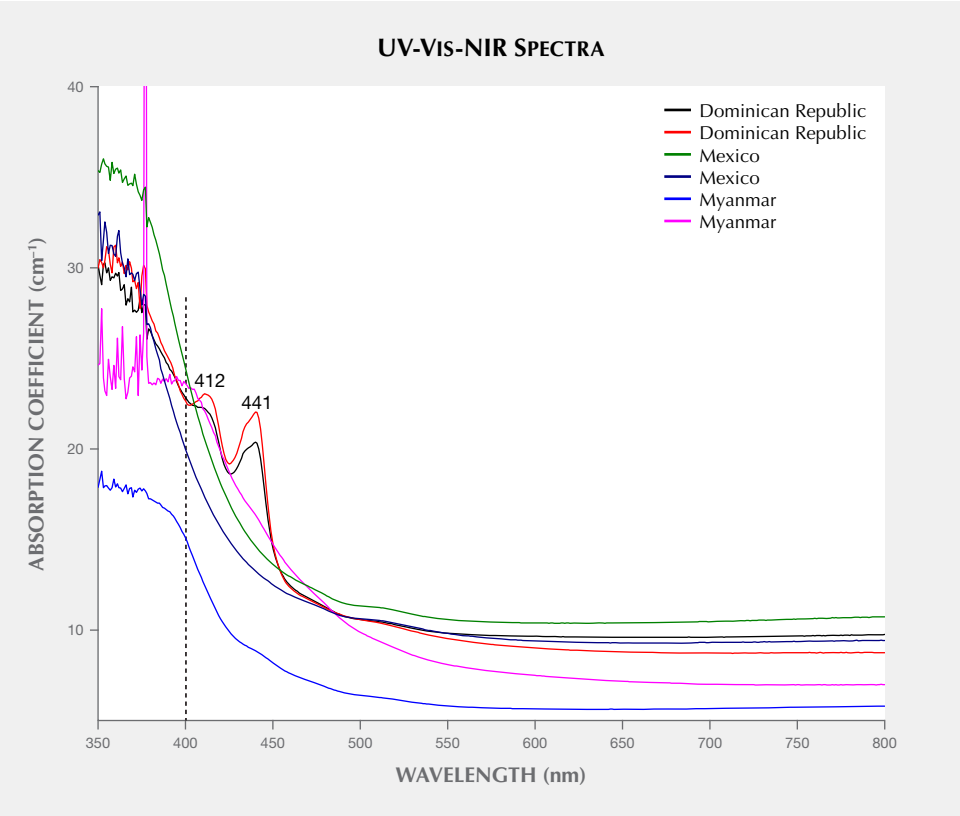

Figure 3. The absorption curves of blue amber from different origins show strong absorbance below 400 nm. While the absorption in the 400–500 nm range varies from origin to origin, the samples from the Dominican Republic showed distinctive absorption peaks at 412 and 441 nm.

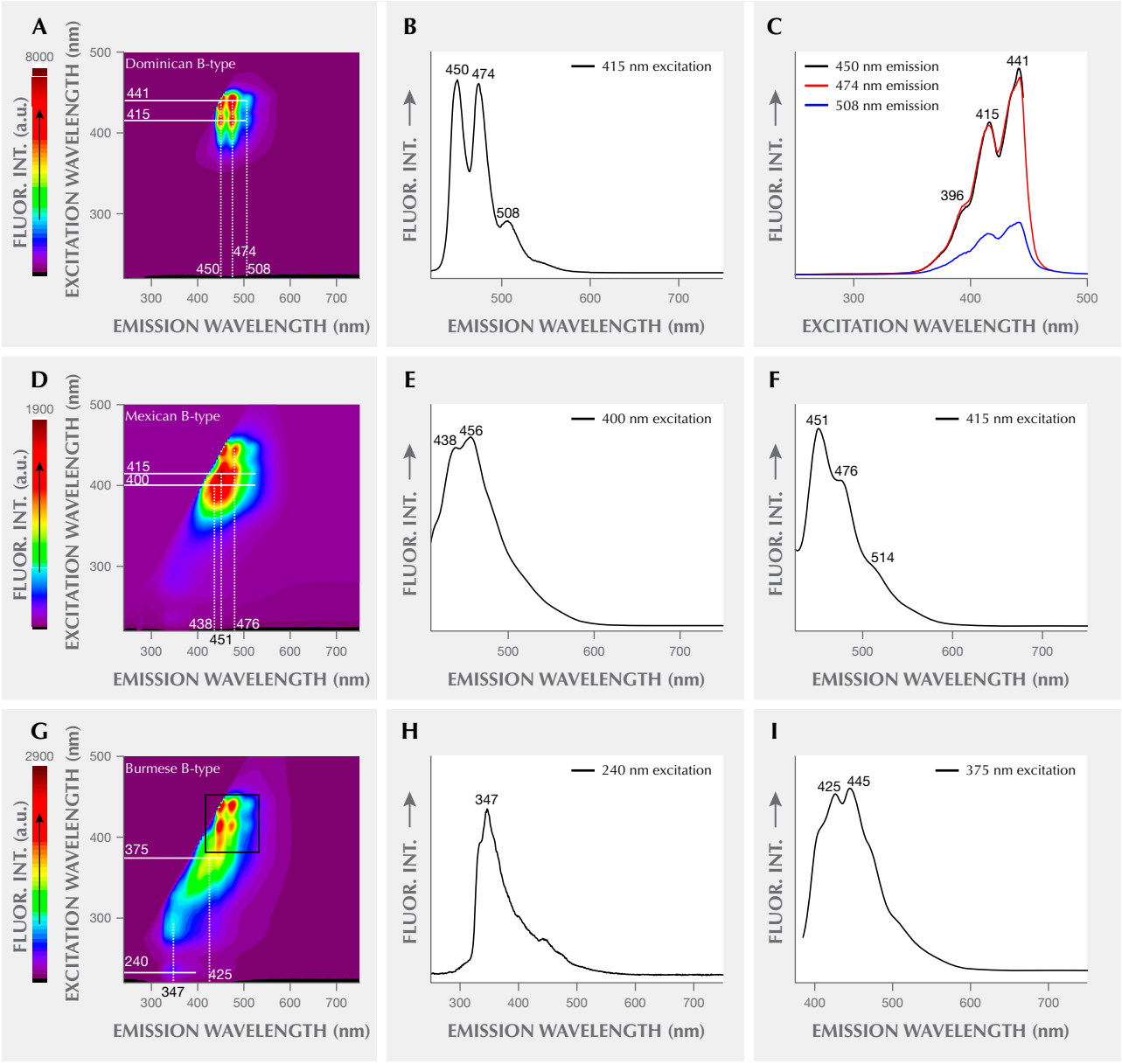

Figure 4. Representative EEMs of B-type amber from three different origins: sample 2 (A–C) from the Dominican Republic, sample 13 (D–F) from Mexico, and sample 17 (G–I) from Myanmar. The left column shows EEM spectra. Images B, E–F, and H–I are emission curves (horizontal sections in EEMs, with λ_{ex} = 415, 400, 375, or 240 nm, as labeled). Image C shows three main excitation curves (as vertical sections in EEMs; different lines are for the different emission peaks). The rectangular area in (G) highlights the EEM area in Burmese B-type sample 17, having a pattern similar to that seen in Dominican B-type amber.

in the very weak to inert fluorescence appearance under SWUV.

In Burmese B-type (seen in figure 4, G–I), a three-emission pattern similar to that of the Dominican B-type was observed in the longer excitation wavelengths (380–450 nm), indicated in figure 4G as the area outlined by a rectangle. The more interesting feature in these samples is in the shorter excitation wavelengths. Two unique emissions were observed: An additional emission peak at about λ_{em} = 425 nm (with a violet color) is at its maximum when excited with λ_{ex} = 375 nm (figure 4I); another λ_{em} at approximately 347 nm (in

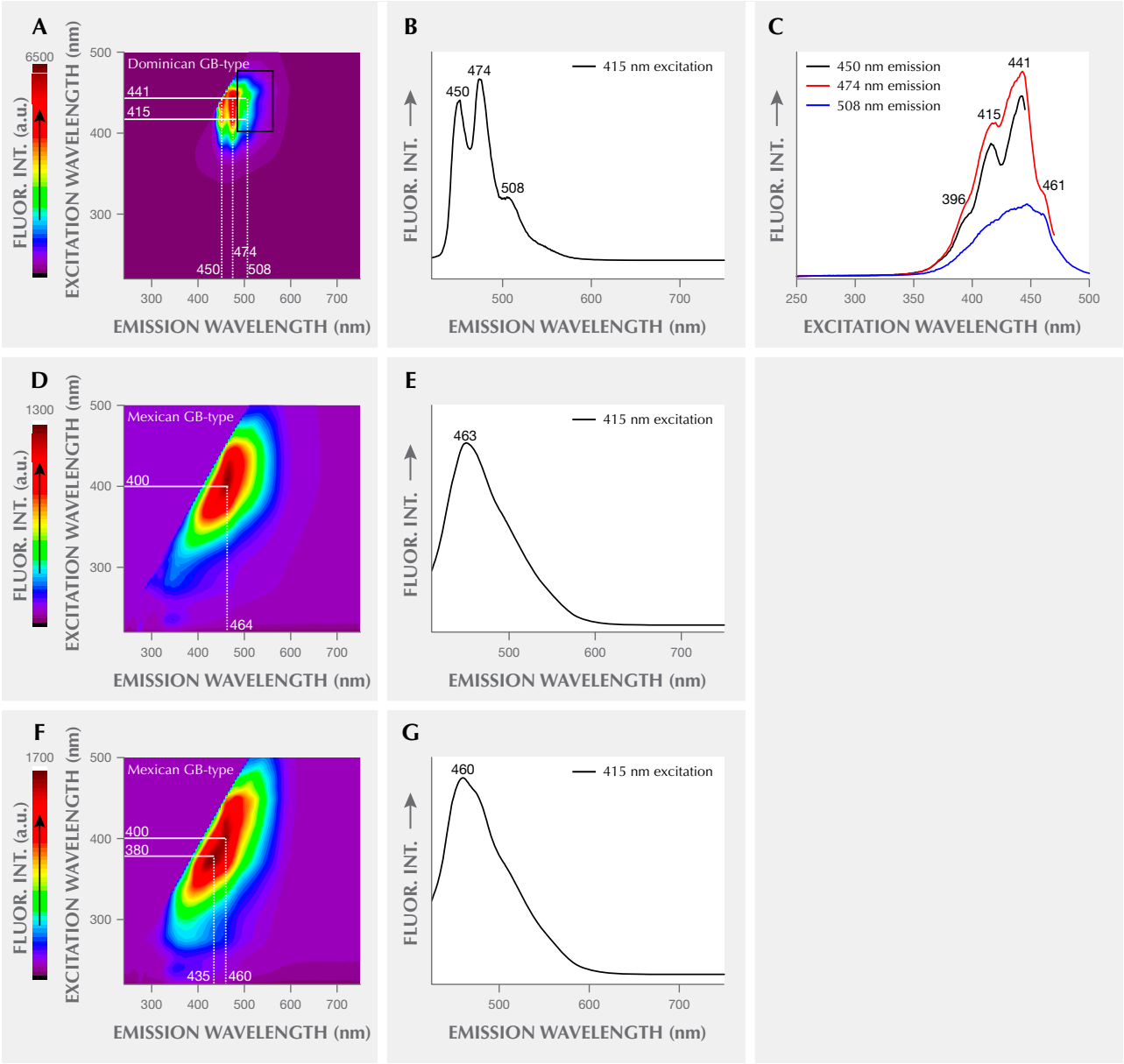

Figure 5. A–C: EEMs and emission and excitation curves show the fluorescence behavior of Dominican GB-type amber, sample 8. The rectangular section in A highlights the additional green fluorescence range. B shows the emission spectrum with λ_{ex} = 415 nm, while C gives the excitation spectra for three different fluorescence emissions, λ_{em} = 450, 474, and 508 nm. The EEMs in D and F and the emission curves with 415 nm excitation in E and G display the fluorescence characteristics of Mexican GB-type amber, samples 15 and 16. Their main emission wavelengths and optimal excitation wavelengths are labeled.

the ultraviolet region) was seen in a wide range of excitation wavelengths, including 240 nm (figure 4H) and from 270 to 330 nm. Again, these spectral features explain the observed weak response to handheld SWUV illumination, especially when compared to the response to LWUV illumination at 365 nm.

Fluorescence of GB-Type Amber. Figure 5 compares the EEM spectra and emission and excitation curves of GB-type amber from the Dominican Republic and Mexico.

In all Dominican GB-type amber, the EEM patterns are similar to those in B-type (for example, fig-

ures 4A and 5A). The major differences include: (1) $I_{\lambda em=474\ nm}$ is much higher than $I_{\lambda em=450\ nm,}$ regardless of the excitation wavelengths, and (2) a longer-wavelength emission tailing toward the green region (indicated by the rectangular area in figure 5A). This tailing varies as the excitation wavelength changes. This emission tailing enhances the green fluorescence, which explains the greener fluorescence appearance in the GB-type amber. Additionally, (3) another excitation extremum at λ_{ex} = 461 nm occurs in excitation curves (figure 5C).

As for Mexican GB-type, the EEMs of samples 15 and 16 (figure 5, D-G) display a broad emission range from the near-ultraviolet to the greenish yellow region (350 to 600 nm), which can be excited with a wide range of excitation wavelengths from 275 to 500 nm. The strongest emission in this material is around 435 nm and/or 464 nm.

Fluorescence of NB-Type Amber. Figure 6 displays the EEM pattern of Dominican NB-type amber. The highest $I_{\lambda em}$ of this amber is only 600, versus the much higher emission counts for B- and GB-type amber, showing maximum values of 8000 to 6500, respectively. This observation indicates that non-blue amber from the Dominican Republic has a much lower fluorescence strength than the other two types from the same locality.

The NB-type amber shows a weak broad emission band in the blue to yellow region (410 to 600 nm) with the highest peak at λ_{em} = 463 nm, best excited by 400 nm light. This is similar to Mexican GB-type amber, but the latter has stronger emission (maximum values of fluorescence intensity are 1300–1700 vs. 600 in Dominican NB-type; see figures 5D and 5F and figure 6A). Due to the wide excitation range and stronger emissions of Mexican GB-type, fluorescence can still be observed visually with sunlight, whereas it cannot in Dominican NB-type (sample 12).

DISCUSSION

In our UV-Vis-NIR absorption spectra (figure 3), the Dominican blue amber showed additional absorption peaks at 412 and 441 nm, which is consistent with the optimal excitation wavelengths for its blue fluorescence. This indicates that Dominican blue amber is very efficient at absorbing these two wavelengths and more likely to generate stronger fluorescence than its Mexican and Burmese counterparts.

When conducting fluorescence measurements, one needs to consider the effects of self-absorption and secondary fluorescence, which can cause errors in fluorescence spectral analysis. These two effects are related—self-absorption occurs when a sample under testing absorbs its own primary fluorescence (Birks, 1974; Lakowicz, 2006) and subsequently emits secondary fluorescence that is either similar to or different from the primary fluorescence. Such absorption may decrease the total amount of fluorescence or reduce a specific peak intensity measured

Figure 6. The 3D fluorescence contour map (A) and emission spectrum (B) of Dominican NB-type amber.

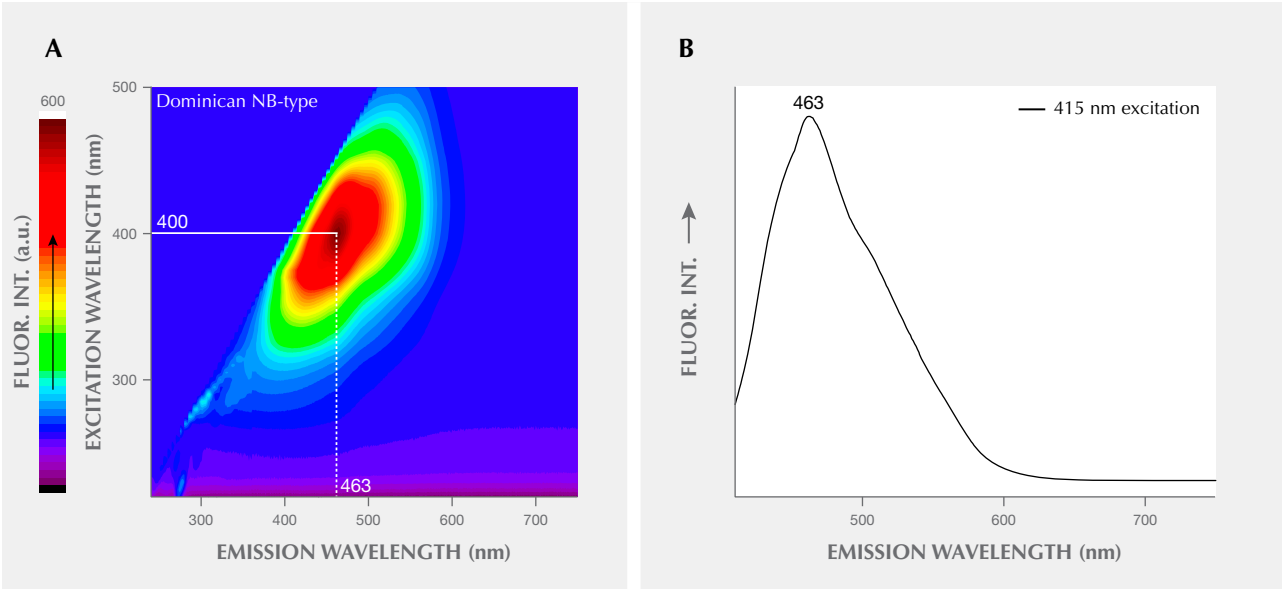

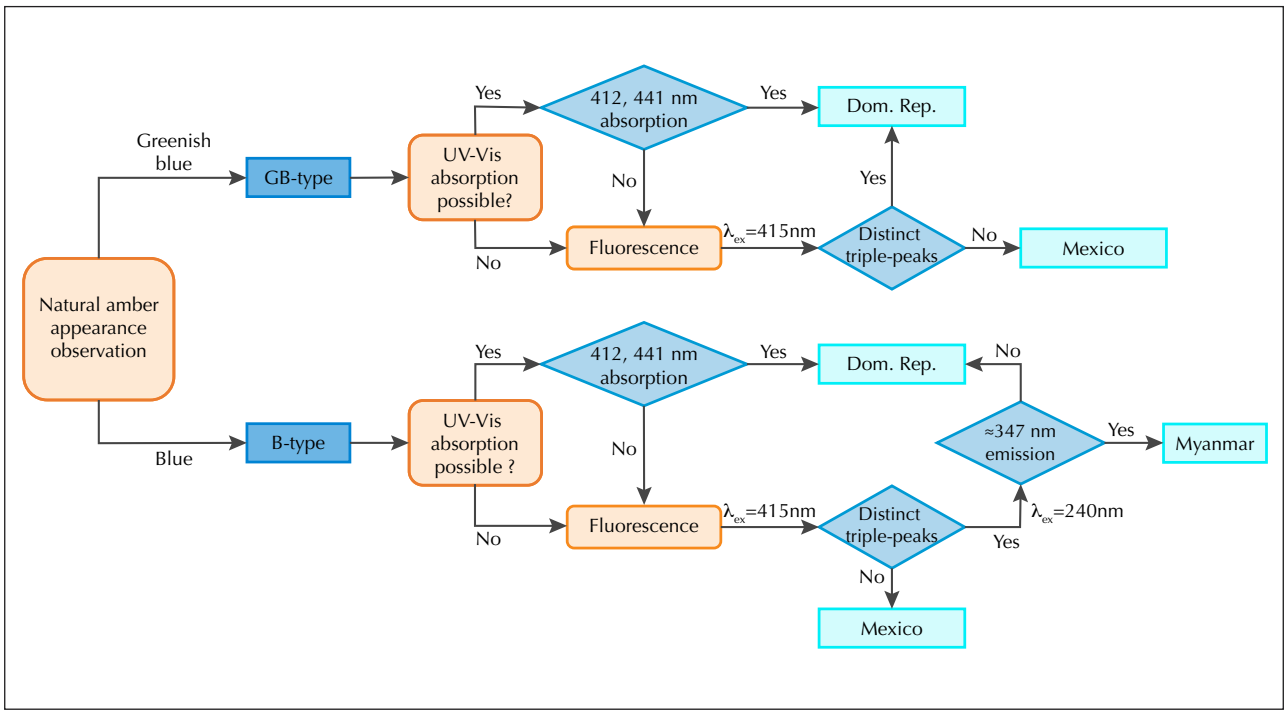

Figure 7. A preliminary flowchart illustrating the combination of visual appearance under D65 light on a black background, UV-Vis-NIR features, and fluorescence features to assist in determining geographic origin of blue amber. Even though clearly Mexican B-type material similarly shows 450, 474, and 508 nm features with 415 nm excitation, this is not a distinct triple peak.

by the instrument, and the secondary fluorescence may produce additional emission peaks or bands. These two effects are more often encountered in a typical fluorescence spectral measurement when the sample is a liquid and loaded in a standard cuvette with 1 cm optical path length. Fortunately, our experiment geometry (as described in box A) can minimize the possibility of self-absorption and secondary fluorescence. Liu et al. (2014) clearly indicated that the fluorescence only occurs on the amber's surface, not deep inside. In addition, our UV-Vis-NIR absorption spectra (figure 3) also showed that any light with wavelength <400 nm will be greatly absorbed and cannot penetrate the amber sample. Thus, the excitation light source is highly unlikely to travel deep into the amber sample to cause self-absorption and secondary fluorescence. Our geometry also ensures that the sample size will not directly influence the amount of fluorescence emission measured.

When we observe amber's fluorescence with the unaided eye, our eyes and brain are extremely sensitive to the fluorescence intensity variations, which allows us to classify the fluorescence response as inert, weak, medium, strong, or very strong. In the current experiment, by strictly controlling the EEM measurement parameters, we achieved a rough quantification of the fluorescence intensity—the intensity bar of the EEM can reflect the relative strength of each sample's fluorescence response. Nevertheless, this procedure may help us set up a future semi-quantitative fluorescence scale for very strong, strong, medium, weak, and inert responses.

Considering the similarities and differences in EEMs from different types of Dominican, Mexican, and Burmese blue amber, it seems possible that EEMs could be aid in separating geographic origin. Figure 7 shows a preliminary flowchart for this separation—by combining the appearance under D65 on a black background, the UV-Vis-NIR absorption (should such test be allowed), and the EEM fluorescence spectra. This summary is based upon the 247 samples we studied and will be further tested and expanded when more samples are available.

Determining the nature of the chemical compound that produces the different fluorescence features is an exceedingly difficult task due to the

structural complicacy resulting from polymerization and the low solubility of amber in most solvents. To date, only Bellani et al. (2005) proposed a possible candidate—perylene—for the triple-peak fluorescence features in Dominican blue amber. Chekryzhov et al. (2014) and Bechtel et al. (2016) excluded perylene for Russian Far East blue amber and proposed azulene ($C_{10}H_8$) as an alternative agent of fluorescence but did not confirm it. Material from the Russian Far East is not commercially available and therefore was not included in this study. Nevertheless, the exact fluorescing agent still has not been successfully extracted, nor has its structure been determined.

CONCLUSIONS

In this study, blue amber refers to amber that shows significant blue fluorescence under a standard D65 light source and, when placed on a black background, this material appears blue to greenish blue. This type of amber is known to come from the Dominican Republic, Mexico, and Myanmar, and material from all three origins exhibits similar gemological properties such as bodycolor, transparency, RI, SG, and internal features. However, their LWUV responses are different—Dominican and Mexican amber mostly show blue fluorescence, while Burmese material displays a violetish blue fluorescence. Blue amber from all three origins showed a similar response to SWUV—much weaker to inert, as compared to the LWUV responses.

We separated blue amber into two types according to their appearance in sunlight or D65 illumination when viewed against a dark background. One is B-type with a blue appearance, and the other is GB-type with a greenish blue appearance. All three origins produce amber that does not show enough blue fluorescence to change its appearance in D65 light; we classified this material as NB-type.

In their EEMs, a triple-peak emission pattern always occurs in Dominican blue amber (both B-type and GB-type). B-type and GB-type Dominican blue amber differ in that the GB-type amber has an additional green fluorescence component (~ 500 nm emission) and an additional 461 nm excitation maximum.

For Mexican B-type amber, the triple-peak features are merged into each other and additional emissions near 438 and 456 nm showed up when using <400 nm excitation. Mexican GB-type amber only has a broad emission feature with an emission center near 460 nm, similar to Dominican NB-type amber. However, Mexican GB-type amber has much stronger emission intensity than Dominican NB-type amber. Burmese B-type amber, in addition to displaying a triple-peak feature similar to Dominican material, has emissions in the violet-ultraviolet region, giving it a violetish appearance.

In the UV-Vis-NIR absorption spectra, in addition to the strong absorption edge just below the near-ultraviolet region (<400 nm) that blue amber from all three sources display, Dominican blue amber has two absorption peaks at 412 and 441 nm, which correspond to the most efficient excitation wavelengths in the EEM. This may explain why Dominican amber fluoresces with much more intensity. Combining the appearance, UV-Vis-NIR spectra, and EEMs, a possible workflow for discriminating blue amber from these three geographic origins is proposed (figure 7). Further study continues to identify the nature of the fluorescing agents and their relationship to the tree species that secrete the specific resins.

ABOUT THE AUTHORS

Ms. Zhang (zhangzhiqing@cug.edu.cn) is a PhD candidate at the Gemmological Institute, China University of Geosciences in Wuhan. Ms. Jiang is a postgraduate student at the Gemmological Institute, China University of Geosciences in Wuhan. Ms. Wang (wangym@cug.edu.cn, corresponding author) is associate professor at the Gemmological Institute, China University of Geosciences in Wuhan, and the director of CUG gem testing center in Guangzhou. Mr. Kong works in the Shenzhen BaoAn Century Amber Museum, China. Dr. Shen (shenxt@cug.edu.cn, corresponding author) is a distinguished professor at the Gemmological Institute, China University of Geosciences in Wuhan.

ACKNOWLEDGMENTS

All authors appreciate the financial support from the National Key R&D program of China (2018YFF0215400) and grants from the Center for Innovative Gem Testing Technology, China University of Geosciences in Wuhan, under grant number CIGTXM-201806. This is contribution CIGTWZ-2020032. The authors are grateful to all the generous merchants for supplying samples. Comments from three anonymous reviewers helped improve this article.

REFERENCES

Airado-Rodriguez D., Durán-Merás I., Galeano-Díaz T., Petter Wold J. (2011) Front-face fluorescence spectroscopy: A new tool for control in the wine industry. *Journal of Food Composition and Analysis*, Vol. 24, No. 2, pp. 257–264.

Bechtel A., Chekryzhov I.Y., Nechaev V.P., Kononov V.V. (2016) Hydrocarbon composition of Russian amber from the Voznovo lignite deposit and Sakhalin Island. *International Journal of Coal Geology*, Vol. 167, pp. 176–183, http://dx.doi.org/10.1016/j.coal.2016.10.005

Bellani V., Giulotto E., Linati L., Sacchi D. (2005) Origin of the blue fluorescence in Dominican amber. *Journal of Applied Physics*, Vol. 97, No. 1, pp. 016101, http://dx.doi.org/10.1063/1.1829395

Berlman I.B. (1971) *Handbook of Fluorescence Spectra of Aromatic Molecules*, 2nd ed. Academic Press, New York and London, 473 pp.

Birks J.B. (1974) Fluorescence parameters and their interpretation. *Journal of Luminescence*, Vol. 9, No. 4, pp. 311–314, http://dx.doi.org/10.1016/0022-2313(74)90044-1

Chekryzhov I.Y., Nechaev V.P., Kononov V.V. (2014) Blue-fluorescing amber from Cenozoic lignite, eastern Sikhote-Alin, Far East Russia: Preliminary results. *International Journal of Coal Geology*, Vol. 132, pp. 6–12, http://dx.doi.org/10.1016/j.coal.2014.07.013

Jiang W., Nie S., Wang Y. (2017) Fluorescence spectral characteristics of blue amber from Dominican Republic, Mexico and Myanmar. *Journal of Gems and Gemmology*, Vol. 19, No. 2, pp. 1–8, http://dx.doi.org/10.15964/j.cnki.027jgg.2017.02.001

Lakowicz J.R. (2006) *Principles of Fluorescence Spectroscopy*, 3rd ed. Springer, Boston, 954 pp, https://doi.org/10.1007/978-0-387-46312-4

Liu Y., Shi G., Wang S. (2014) Color phenomena of blue amber. *G&G*, Vol. 50, No. 2, pp. 134–140, http://dx.doi.org/10.5741/GEMS.50.2.134

Matuszewska A., Czaja M. (2002) Aromatic compounds in molecular phase of Baltic amber—synchronous luminescence analysis. *Talanta*, Vol. 56, No. 6, pp. 1049–1059, http://dx.doi.org/10.1016/S0039-9140(01)00610-5

Mysiura I., Kalantaryan O., Kononenko S., Zhurenko V., Chishkala V., Azarenkov M. (2017) Ukrainian amber luminescence induced by X-rays and ultraviolet radiation. *Journal of Luminescence*, Vol. 188, pp. 319–322, http://dx.doi.org/10.1016/j.jlumin.2017.04.045

Parker C.A. (1968) Apparatus and experimental methods. In C.A. Parker, Ed., *Photoluminescence of Solutions with Applications to Photochemistry and Analytical Chemistry*. Elsevier, Amsterdam, pp. 128–302.